27. Clancy BM, Czech MP. Hexose transport stimulation and membrane redistribution of glucose transporter isoforms in response to cholera toxin, dibutyryl cyclic AMP and insulin in 3T3 adipocytes. *J Biol Chem* 1990;265:12434–12443.
28. Hariharan R, Bray M, Ganim R, Doenst T, Goodwin GW, Taegtmayer H. Fundamental limitations of (18F)2-deoxy-2-fluoro-D-glucose for assessing myocardial glucose uptake. *Circulation* 1995;91:2435–2444.
29. Kubota K, Ishiwata K, Kubota R, et al. Tracer feasibility for monitoring tumor radiotherapy: a quadruple tracer study with fluorine-18-fluorodeoxyglucose or fluorine-18-fluorodeoxyuridine, L-[methyl-14C]methionine, [6-3H]thymidine and gallium-67. *J Nucl Med* 1991;32:2118–2123.
30. Christensen HN. Role of amino acid transport and countertransport in nutrition and metabolism. *Physiol Rev* 1990;70:43–76.
31. Conti PS, Sordillo EM, Sordillo PP, Schmall B. Tumor localization of alpha-aminoisobutyric acid (AIB) in human melanoma heterotransplants. *Eur J Nucl Med* 1985;10:45–47.
32. Dunzendorfer U, Schmall B, Bigler RE, et al. Synthesis and body distribution of alpha-aminoisobutyric acid-11C in normal and prostate cancer bearing rat after chemotherapy. *Eur J Nucl Med* 1981;6:535–538.
33. Scanlon K, Safirstein RL, Thies H, Gross RB, Waxman S, Guttenplan JB. Inhibition of amino acid transport by cis-diaminedichloroplatinum (II) derivatives L1210 murine leukemia cells. *Cancer Res* 1983;43:4211–4215.
34. Scanlon K, Cashmore AR, Kashani-Sabet M, et al. Inhibition of methionine uptake by methotrexate in mouse leukemia L1210. *Cancer Chemother Pharmacol* 1987;19:21–24.
35. Hoffman RM. Altered methionine metabolism and transmethylation in cancer. *Anticancer Res* 1985;5:1–30.
36. Higashi K, Clavo AC, Wahl RL. Does FDG uptake measure the proliferative activity of human cancer cells? In vitro comparison with DNA flow cytometry and tritiated thymidine uptake. *J Nucl Med* 1993;34:414–418.

Preclinical Studies of Indium-111-Labeled IgM: A Human Monoclonal Antibody for Infection Imaging

Ramaswamy Subramanian, Shankar Vallabhajoshula, Helena Lipszyc, Quing Zhao, James Murray, Samir Shaban, Josef Machac and Michael G. Hanna, Jr.

PerImmune, Inc., Rockville, Maryland; Division of Nuclear Medicine, Department of Radiology, The Mount Sinai Medical Center, New York, New York

Indium-111-labeled plasma proteins, such as albumin, transferrin and IgG, have been proven useful to image infection. We reported previously that 111In-labeled human monoclonal antibody, IgM 16.88 (In-IgM) also would localize at the site of infection. However, the kinetics of blood clearance, distribution and infection uptake have not been investigated. We compared the kinetics of distribution and infection uptake of In-IgM 16.88 with that of In-polyclonal IgG in rats with focal infection. **Methods:** Both IgM 16.88 and polyclonal IgG were labeled with 111In using a bifunctional chelating agent, LiLo. The labeling efficiency was >95%. Focal infection was induced in rats by an intramuscular injection of E. Coli in the right thigh. In-IgM (30–40 μCi) was injected into five groups of rats (five rats/group). The rats were killed at 4, 8, 16, 24 and 36 hr. The percent injected dose (%ID) in blood, infection muscle, control muscle, liver, spleen and kidney were determined. Similar studies were performed with In-IgG. **Results:** The In-IgM activity in blood at 4 hr postinjection was 27% which decreased to 2% by 36 hr. In contrast, the In-IgG blood activity was 40% at 4 hr and 20% at 36 hr. The infection/muscle (I/M) ratios are higher with In-IgM at all time points postinjection compared to that of In-IgG. At 24 hr, the I/M ratio was 22 compared to 9 with In-IgG. At the same time point, the infection/blood (I/B) ratio with In-IgM was 2.7 compared to only 0.8 with that of In-IgG. In-IgM was taken up mostly by the liver compared to diffuse abdominal uptake of IgG. **Conclusion:** These results indicate that In-IgM produces higher lesion to background ratio when compared to In-IgG and, therefore, is potentially useful to image infection in patients.

Key Words: IgM; indium-111; infection imaging; LiLo; 16.88; human monoclonal antibody

J Nucl Med 1997; 38:1054–1059

The most commonly used radiotracers for imaging occult infection in patients are 67Ga-citrate and radiolabeled (111In or 99mTc) leukocytes (1,2). Although these agents have been shown to be efficacious, several new tracers are being evaluated as potential infection imaging agents. Radiolabeled human

polyclonal IgG and liposomes labeled with 111In or 99mTc have shown potential diagnostic use in experimental infection models (2–6). In addition, several radiolabeled chemotactic peptides also are being evaluated as radiotracers for infection imaging studies (7–9). Due to slow blood clearance of labeled IgG, the target/background and target/blood ratios are suboptimal and delayed imaging at 24 and 48 hr are essential for good quality images. On the other hand, the labeled peptides clear very rapidly from circulation, but the absolute uptake at the site of infection is very low. The mechanism(s) of localization of radiolabeled proteins appears to be nonspecific and the localization is due mostly to increased capillary permeability and extravascular leakage (1–4).

We have developed a human monoclonal antibody belonging to IgM class, designated as IgM 16.88 which can be radiolabeled with 111In using the bifunctional chelating agent LiLo, 1,3-bis[N-N(2-aminoethyl)–2-aminoethyl]–2-aminoacetamido]–2-(4-isothiocyanatobenzyl)propane-N,N,N',N'',N''',N'''',N''''',N''''''-octaacetic acid. We have reported previously that this agent has very high in vitro and in vivo stability (10,11). Preliminary immunohistopathological studies have shown that the LiLo-IgM 16.88 conjugate binds almost exclusively to the dead white blood cells (granulocytes and lymphocytes) while binding to live cells (and red blood cells) was minimal. In a preliminary study, we also observed that 111In-labeled LiLo-IgM 16.88 localizes in the site of experimental infection in rats and that the image quality was better than with 111In-labeled polyclonal and monoclonal IgG preparations (12,13). In order to assess the potential diagnostic use of 111In-LiLo-IgM 16.88 as a tracer to image occult infection, we compared the kinetics of distribution and infection uptake of 111In-LiLo-IgM 16.88 with that of 111In-LiLo-polyclonal human IgG preparation in rats and rabbits with focal infection (14). The results presented here clearly demonstrate that the infection/muscle and infection/blood ratios with In-IgM are significantly higher than with In-IgG.

MATERIALS AND METHODS

LiLo is a bifunctional chelating agent, 1,3-bis[N-N(2-aminoethyl)−2-aminoethyl]−2-aminoacetamido]−2-(4-isothiocyanatobenzyl)propane-N,N,N',N'',N''',N'''',N''''',N''''''-octaacetic acid, suitable for attaching radiometals such as ^{111}In and ^{90}Y to proteins. Detailed synthetic procedures, spectral characterizations for LiLo and procedure for coupling LiLo to monoclonal antibodies have been described elsewhere (11).

Antibodies

The human monoclonal antibody 16.88 (IgM isotype) was produced by Epstein Barr Virus transformed human lymphoblastoid cell lines derived from the peripheral blood lymphocytes of colon carcinoma patients (15). These patients were specifically immunized with autologous tumor cells as part of an active specific immunotherapy clinical protocol (16). Immunohistochemical analysis has indicated that 16.88 reacts with epitopes on a unique molecular structure as well as shared epitopes with cytokeratins 8, 18 and 19 (17).

Radiolabeling

The nonspecific polyclonal human IgG and human monoclonal antibody IgM 16.88 were first coupled to the bifunctional chelating agent, LiLo and subsequent radiolabeling with ^{111}In was performed as described previously (11,18). In brief, 0.1 ml of antibody-LiLo conjugate (0.6−0.8 mg) in phosphate buffered saline solution (pH 7.2) was added to ^{111}In-chloride in a mixture (1:1 v/v) of acetate solution, 0.6 M, pH 5.5, and citrate solution 0.06 M, pH 5.5. The reaction mixture was incubated at room temperature for 30−45 min and an aliquot of DTPA solution was added to scavenge the excess unbound ^{111}In. The reaction mixture was further purified by gel filtration column chromatography.

The percentage of ^{111}In bound to the antibody was determined using ascending thin-layer chromatography (solvent system: 50/50 mixture of 0.1 M acetate solution and methanol) or ITLC-SG strips (solvent system: phosphate buffered saline solution, 0.05 M, pH 7.2). In all cases the radiolabeling efficiency (the amount of ^{111}In bound to IgM or IgG) was greater than 95%. We have shown previously that ^{111}In-LiLo-antibody preparations were stable in buffer solution as well as in serum for more than 72 hr (11).

Animal Model

An acute focal infection model was used to compare the kinetics of ^{111}In-IgM with that of ^{111}In-IgG. The same animal model was used by several investigators to study the uptake of radiolabeled proteins and peptides at sites of infection (3,7,9). The E. Coli bacteria obtained from a clinical isolate was grown for 24 hr on trypitase soy agar plates. A bacterial cell suspension in saline was then made containing 4×10^7 bacteria/ml that was mixed with an equal volume of heparinized rat blood. Male rats (150–200 g) were injected in the right thigh muscle with 0.1 ml of the cell suspension containing 2×10^6 E. Coli while the left leg served as a control. The rats developed severe focal infection within 24 hr as indicated by swelling of the right thigh. Similar focal infection in the thigh muscle was also induced in male New Zealand white rabbits (2–3 kg) within 24 hr following an injection of 0.5 ml of E. Coli cell suspension mixed with an equal volume of rabbit blood.

Biodistribution of Indium-111-Labeled IgM and IgG in Rats

Twenty-five infected rats were injected through the tail vein with 50–70 μCi of ^{111}In-LiLo-IgM 16.88 (In-IgM) preparation (0.1 mg, 0.25 ml). To study the kinetics of biodistribution and infection uptake, the 25 rats were divided into five groups of five rats each. At different times postinjection, 4, 8, 16, 24 and 36 hr, a group of rats was killed. Various tissue samples (infected muscle, control muscle, blood, liver, kidney and spleen) were taken. The samples were weighed and counted in a gamma well counter along with a

standard (prepared from the injection mixture). The ^{111}In activity in the tissues was expressed as a percent of injected radioactive dose (%ID or %ID per gram). Similar biodistribution studies were performed in another group of 25 infected rats using ^{111}In-LiLo-IgG (In-IgG) preparation.

Imaging Studies

To evaluate and compare the image quality of In-IgM with that of In-IgG, a group of four infected rabbits was injected with 200 μCi of In-IgM (0.4 mg) while an additional group of four rabbits was injected with In-IgG. Whole-body images of the rabbits were obtained using a gamma camera fitted with a medium-energy collimator. The rabbits were anesthetized using a mixture of ketamine and rompun. Anterior whole-body images were acquired for 15 min using a 256 × 256 matrix. The images were acquired at 4 hr and again at 24 hr following injection of radioactivity. At 24 hr, after imaging studies, the rabbits were killed and the %ID in the infection muscle, control muscle and blood were determined.

Immunohistochemical Studies

To assess the extent of IgM 16.88 binding to granulocytes and lymphocytes, either in circulation or at the infection site, immunohistochemical studies were performed with white blood cells (WBCs) isolated from human blood. The leukocyte populations were obtained from four healthy volunteers (three women and one man representing the four major ABO blood groups) by venipuncture, into EDTA containing Vacutainer tubes. The cells were separated into mononuclear cells (lymphocytes and monocytes) and granulocytes using a mixture of Histopaque 1077 (Sigma, St. Louis, MO) per the manufacturer's instructions.

Live-Cell Fluorescence. An indirect immunofluorescence protocol was used in which ficoll hypaque separated granulocytes and mononuclear cells (lymphocytes and monocytes) were reacted first with LiLo-16.88. The cells were then reacted with a flourescein isothiocyanate (FITC) conjugated antihuman IgM (20 μg/ml; Tago, Burlingame, CA). Dead cells were indicated by the uptake of propidium iodide into the nucleus. Fluorescence activity was determined microscopically using a Zeiss microscope equipped with an FL epi-fluorescence condenser. The granulocyte population contained a moderate amount of red blood cells (RBC), allowing evaluation of the reactivity of 16.88 with RBCs concurrently with the granulocyte population. Additionally, we used a buffer control (RPMI 1640 + 10% fetal bovine serum, FBS) to control for background binding of the FITC conjugate to the leukocytes as well as a negative control antibody (normal human polyclonal IgM).

Fixed-Cell Fluorescence. Briefly, before leukocytes were reacted with IgM antibodies, they were pelleted by centrifuging at 200 × g for 5–10 min. The cells were washed in protein-free HBSS and then fixed with ice cold acetone for 5 min followed by washes with HBSS and then RPMI-1640 + 10% FBS. From this point, the staining procedure was the same as described for the live-cell fluorescence assay.

RESULTS

Blood Clearance

Following intravenous administration of ^{111}In-labeled immunoglobulins, the %ID in whole blood as a function of time is shown in Table 1. In addition, the time-activity curves for both tracers are shown in Figure 1A. At 4 hr, the amount of In-IgM in circulation (27%) was significantly less than that of In-IgG (40%), and the rate of In-IgM clearance from circulation was more rapid than that of In-IgG. At 36 hr, only 2% of In-IgM was still in circulation compared to 20% of In-IgG.

		% Injected dose/organ			
	Time	Blood	Liver	Spleen	Kidney
In-IgM 16.88	4 hr	26.57 ± 2.42	27.95 ± 1.69	1.18 ± 0.13	1.49 ± 0.15
	8 hr	16.45 ± 2.18	37.85 ± 1.92	1.38 ± 0.15	1.58 ± 0.19
	16 hr	6.99 ± 2.08	36.07 ± 7.45	1.34 ± 0.29	1.10 ± 0.11
	24 hr	4.74 ± 0.68	35.37 ± 4.84	1.31 ± 0.39	1.31 ± 0.039
	36 hr	2.2 ± 0.65	38.77 ± 4.48	1.47 ± 0.30	1.27 ± 0.067
In-IgG	4 hr	39.75 ± 2.24	12.40 ± 1.68	0.92 ± 0.11	8.63 ± 1.04
	8 hr	30.96 ± 8.36	10.23 ± 2.74	0.79 ± 0.24	9.34 ± 1.78
	16 hr	23.21 ± 2.14	9.75 ± 1.46	0.77 ± 0.23	10.01 ± 1.00
	24 hr	21.058 ± 0.74	9.13 ± 1.38	0.75 ± 0.097	11.54 ± 0.97
	36 hr	20.09 ± 0.73	11.76 ± 0.77	0.79 ± 0.049	11.41 ± 0.54

Infection Uptake Kinetics

The kinetics of In-IgM and In-IgG uptake and retention in the infectious muscle and the control muscle is shown in Figure 1B and C. At 4 hr in the infectious muscle, the %ID/g of In-IgM (0.63 ± 0.07) was significantly less than that of In-IgG (1.12 ± 0.31). The maximum uptake with In-IgM was 1.02% ID/g at 8 hr, and over the next 28 hr, the activity gradually decreased to 0.76% ID/g while the In-IgG activity at the site of infection was relatively constant during the same time period. In the control muscle (Fig. 1C), the uptake of In-IgM was significantly lower than In-IgG; 0.046 versus 0.11% ID/g at 8 hr and 0.038 versus 0.13% ID/g at 36 hr.

The two important parameters describing the image quality of a radiotracer are target/background (muscle) and target/blood ratios. The relative change in the magnitude of these two ratios with In-IgM and In-IgG as a function of time, are shown in Figure 2A and B. At 4 hr, the infection/muscle (I/M) ratio with IgM was slightly higher (Fig. 2A) compared with that of IgG (14 versus 11). At later time points, this ratio increased significantly with IgM while there was not much change with IgG (22 versus 9.4 at 24 hr). The infection/blood (I/B) ratios with In-IgM (Fig. 2B) and In-IgG were similar at 4 hr (around 0.4). This ratio increased significantly with IgM to 5.5 at 36 hr while In-IgG only showed a small increase.

Biodistribution

The kinetics of distribution and uptake of In-IgM and IgG in the infected rats is provided in Table 1. The liver sequesters most of In-IgM activity. At 8 hr, 38% of In-IgM was taken up by the liver and only 1%–2% by the kidneys and spleen. By contrast, the liver and kidney uptake of In-IgG was about 10% each and spleen uptake was <1%. Over the next 48 hr, however, there was essentially no difference between In-IgM and In-IgG in the net accumulation of radioactivity in these organs.

Imaging Studies

The gamma camera images showing the biodistribution and infection uptake at 4 and 24 hr postinjection of In-IgM and In-IgG in rabbits with focal infection are presented in Figure 3. Infection in the leg can be seen as early as 4 hr postinjection of In-IgM whereas, in the case of In-IgG, the localization is seen at 24 hr postinjection. Background blood pool activity is relatively less with In-IgM when compared to In-IgG.

Immunohistochemistry

The reactivity of the LiLo-IgM 16.88 conjugate with live and dead lymphocytes and granulocytes is presented in Table 2. The reactivity of the LiLo-IgM 16.88 conjugate was compared with that of a negative control as described in the Materials and Methods section. The viability of all cell populations was
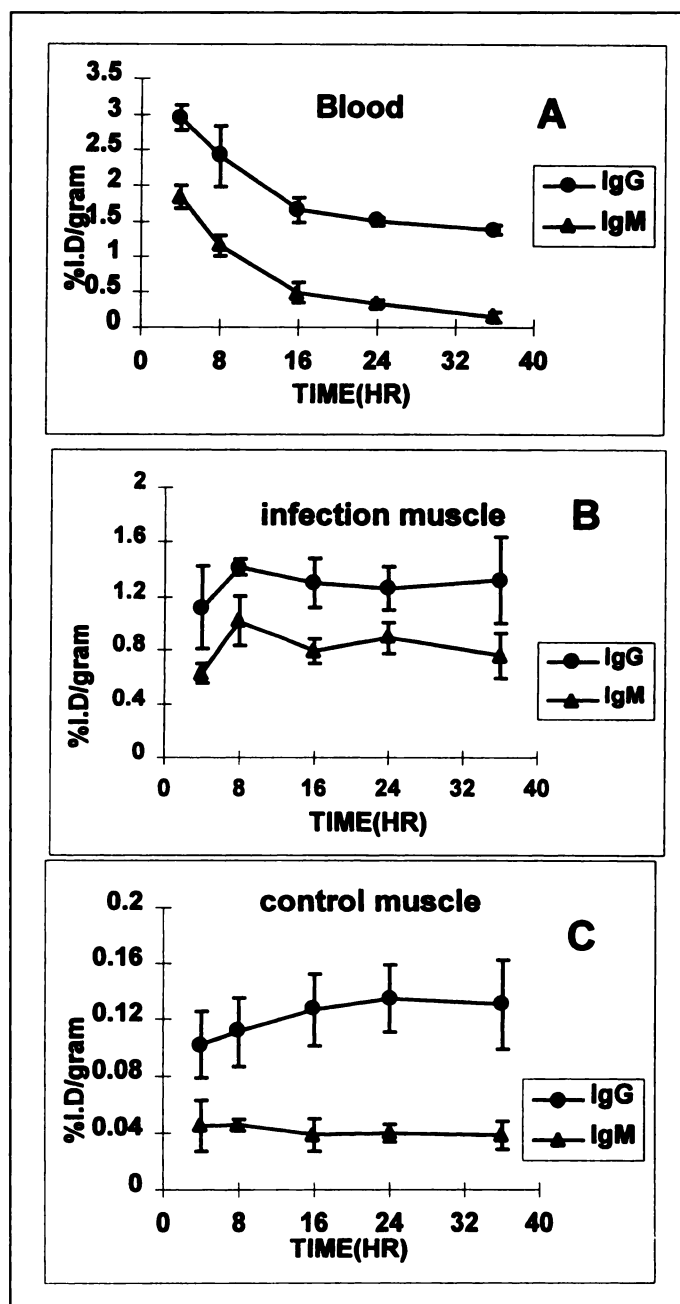

FIGURE 1. In rats with focal infection, the pharmacokinetics of ^{111}In-labeled LiLo-IgM 16.88 and LiLo-polyclonal IgG are shown as a percent of injected dose (% ID/g) in (A) blood, (B) infection muscle and (C) control muscle.
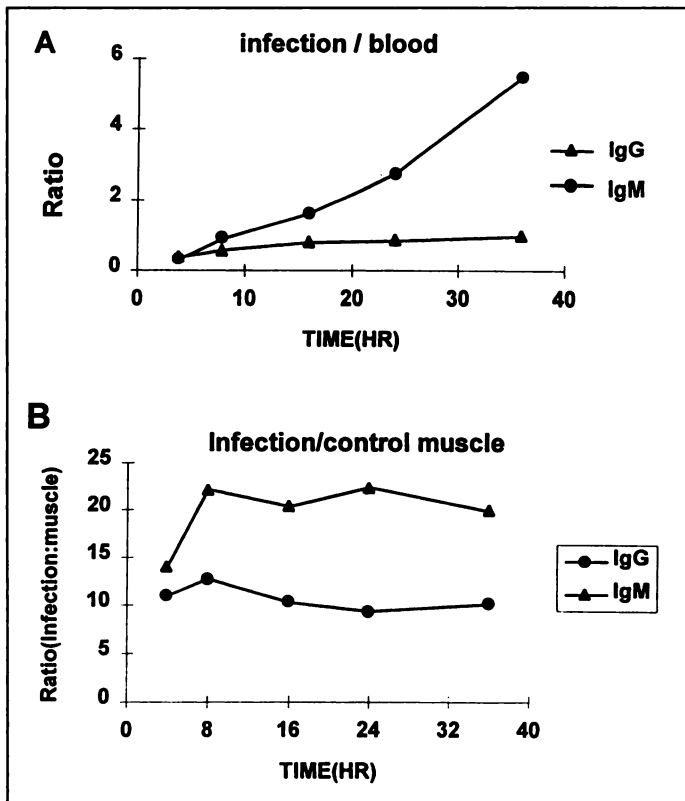
FIGURE 2. In rats with focal infection, the dynamics of ^{111}In-labeled LiLo-IgM 16.88 and LiLo-polyclonal IgG are shown as (A) infection/blood and (B) infection/muscle ratios.

>98% and was judged by exclusion of the nuclear stain, propidium iodide (data not shown).

The reactivity of the LiLo-16.88 conjugate was similar to that of the negative control IgM with live lymphocytes ($\leq$7%) and with live granulocytes ($\leq$1%). In contrast, the LiLo-IgM 16.88 conjugate reacted with 100% of the dead lymphocytes and granulocytes while the negative control IgM was unreactive.

DISCUSSION

In the present investigation, we evaluated the diagnostic potential of radiolabeled, totally human IgM isotype monoclonal antibody, 16.88 to detect infection in vivo. There are several reasons for evaluating the IgM monoclonal antibody. We were able to show previously that human monoclonal antibodies can be produced in large amounts and can be chemically modified without destroying the immunoreactivity of the protein (11). It has been reported that the biological half-life of IgM antibodies is 5 days compared to the 23-day half-life of IgG antibodies (19). Hence, it is expected that the plasma clearance of ^{111}In-labeled IgM would be faster than that of ^{111}In-IgG. In addition, immunohistochemical studies have shown that IgM 16.88 antibody binds selectively to dead granulocytes and lymphocytes but not to the live cells. Human polyclonal IgM, on the other hand, shows no reactivity to either live or dead granulocytes and lymphocytes. Based on this observation, we suspected that ^{111}In-LiLo-IgM might bind to the damaged WBCs at the infection site. In order to validate this hypothesis, we compared the kinetics of distribution and infection uptake of these two tracers (In-IgM and In-IgG) in an animal model of acute infection induced in rats by injection of E. Coli bacteria in the thigh muscle.

Results demonstrate that ^{111}In-labeled 16.88-LiLo clears from the circulation faster than In-IgG (Fig. 1A). At 24 hr, 5% of the injected dose of In-IgM was in circulation compared to 21% of the injected dose with In-IgG. This rapid blood clearance produces a dramatic difference in the infection/blood ratios (I/B) of these two tracers. Initially, at 4 hr, both tracers have similar I/B ratios (about 0.35), but by 24 hr, In-IgM shows an 8-fold increase in ratio (2.74) compared to only a 2-fold increase by In-IgG (0.84). Clonal variation in carbohydrate composition of the antibodies produced in tissue culture or labeling and purification methods may accelerate the metabolism of the antibodies (20). A similar fast clearance of 16.88 has been observed earlier (21,22).

One of the major advantages of In-IgM 16.88 appears to be that the liver is the major organ accumulating In-IgM activity in the abdomen while the activity in the spleen and kidneys was
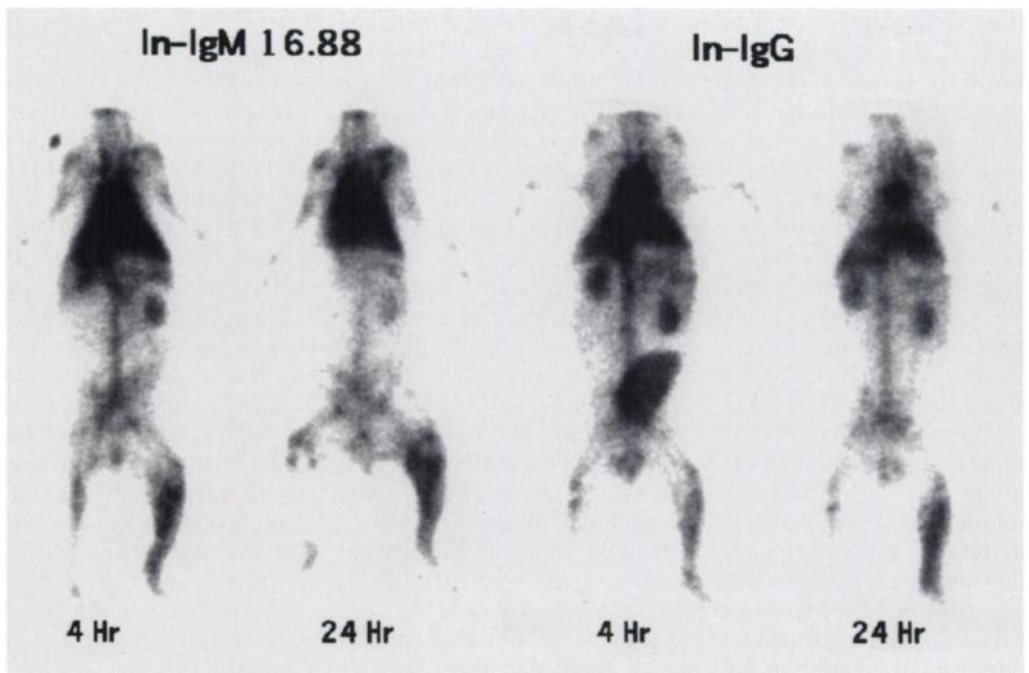

FIGURE 3. Gamma camera images at 4 hr and 24 hr showing in vivo distribution and infection uptake in rabbits with focal infection after administration of ^{111}In-labeled LiLo-IgM 16.88 and LiLo-polyclonal IgG. I = infection.

TABLE 2

Reactivity of LiLo-16.88 with Live and Fixed Normal Human Lymphocytes/Granulocytes as Determined by Indirect Immunofluorescence

A. Live			Lymphocytes			Granulocytes		
Donor	Blood group	Antibody	Total cells counted	Cells stained	Average intensity	Total cells counted	Cells stained	Average intensity§
		Negative control*	254	7.1%	3+	303	0%	0
1	A	LiLo-16.88	215	6.0%	2+	250	0%	0
		Negative control	225	3.1%	2–3+	235	0%	0
2	B	LiLo-16.88	294	4.4%	2+	291	0%	0
		Negative control	234	3.0%	1+	288	0%	0
3	AB	LiLo-16.88	258	5.1%	1–2+	310	0%	0
		Negative control	231	3.4%	1+	278	1%	1–2+
4	O	LiLo-16.88	272	5.9%	1–3+	361	<1%	1–2+
B. Fixed								
		Negative control	>200†	0%	0	>200‡	0%	
1	A	LiLo-16.88	184	100%	4+	>200‡	~100%‡	4+
		Negative control	189	0%	0	>200‡	0%	
2	B	LiLo-16.88	201	100%	4+	>200‡	~100%‡	4+
		Negative control	205	0%	0	>200‡	0%	0
3	AB	LiLo-16.88	274	100%	4+	>200‡	~100%‡	4+
		Negative control	193	0%	0	>200‡	0%	0
4	O	LiLo-16.88	171	100%	4+	>200‡	~100%‡	4+

*Negative control was normal human IgM.

†Looked at more than six fields of 40+ lymphocytes per field. There were considerable numbers of free nucleus (no cytoplasm apparent). Cells that had detectable cytoplasm were not stained by the negative control IgM.

‡Cells were significantly clumped making an individual count impossible. Cell number and percent stained were estimated.

§Staining intensity was evaluated on a 0 to 4+ scale with 0 = no staining; 1+ = weak staining; 2+ = moderate staining; 3+ = strong staining and 4+ = very strong staining.

insignificant (2 %ID). In contrast, the localization of In-IgG in the abdomen is relatively diffuse (Table 1). The higher uptake of radiolabeled IgM in the liver has been observed earlier by other investigators (23).

The absolute uptake of In-IgM in the infection muscle was less than that of In-IgG (Fig. 1B). This decreased infection uptake of In-IgM might be due to decreased absolute amount (%ID/ml in blood) and retention of activity in blood. More importantly, the relative uptake of In-IgM in the control muscle was also less than that of In-IgG (Fig. 1C). As a result, the infection/muscle (I/M) ratios with In-IgM are almost two times higher compared to that of In-IgG at 8 hr postinjection (I/M ratio of 22 for In-IgM compared to 13 for that of In-IgG). Previous studies in the same rat infection model have shown that In-IgG and In-HSA had I/M ratios of about 9 at 24 hr postinjection (24). The present investigation demonstrates that with In-IgM we can obtain I/M ratios of about 20 even as early as 8 hr after injection.

The imaging studies performed in rabbits bearing E. Coli infection further confirmed these observations. In the case of IgM, infection can be visualized as early as 4 hr postinjection whereas, with IgG, the image quality was poor at early time points. At 24 hr postinjection, the blood-pool activity was much lower for IgM than in the case of IgG. Higher uptake in liver was seen for 16.88 at all time points.

There are some plausible explanations for the infection uptake and retention of the In-IgM monoclonal antibody. IgM 16.88 is a human monoclonal antibody recognizing a colon tumor-associated antigen, designated CTAA-16.88 (apparent avidity in the range of 5 × 10⁸ l/M) (25). Based on biochemical and immunologic evidence, this antigen is reported to be an altered form of intermediate filament proteins (17). It has been previously demonstrated that certain intermediate filament proteins are susceptible to proteolytic degradation that results in

smaller yet discrete proteins. In addition, it has been shown that there are increases in proteolytic activity that accompany abscess formation or bacterial and other infections. The IgM 16.88 has been tested for its reactivity with live lymphocytes, granulocytes and a series of intermediate filament proteins. The 16.88 does not react with live lymphocytes and granulocytes; however, the IgM 16.88 antibody reacted with dead lymphocytes and granulocytes (17). These observations suggest that In-IgM 16.88 might bind to damaged WBCs at the site of infection. Additional studies are underway to elucidate the mechanism of localization of 16.88 at the site of infection.

CONCLUSION

Indium-111-LiLo-IgM 16.88 has been shown to be safe for human use. In several clinical studies involving IgM 16.88 labeled with ¹³¹I, ¹¹¹In and ¹⁸⁶Re, no detectable levels of human antihuman antibody (HAHA) were detected (26,27). Murine-derived antigranulocyte antibodies, although reported to localize well at infectious foci, have the potential to elicit immune responses leading to formation of human antimurine monoclonal antibodies (HAMA) that makes repeat infusions difficult. Earlier dosimetry calculations, on the basis of mice biodistribution studies to estimate radiation dose to patients, did not exceed 1.5 rad to any organ per mCi of ¹¹¹In-LiLo-16.88 (10).

Fast background clearance and improved target-to-nontarget ratios are important factors for consideration while designing a radiopharmaceutical. These results demonstrate that the human monoclonal antibody 16.88 may be useful in imaging infectious foci. Since this agent accumulates in the liver to a considerable extent, imaging of infections in the upper abdomen and lower chest area may be difficult. Even when use has to be limited to the extremities in infectious bone and joint disease, the performance of 16.88 is more than promising. Indium-111-labeled 16.88-LiLo is currently under clinical evaluation.

REFERENCES

1. Pike CP. Imaging of inflammatory sites in the 1990s: new horizons [Editorial]. *J Nucl Med* 1991;32:2034–2036.
2. Datz FL, Morton KA. New radiopharmaceuticals for detecting infection. *Invest Radiol* 1993;28:356–365.
3. Fischman AJ, Rubin RH, Khaw BA, et al. Detection of acute inflammation with ^{111}In-labeled nonspecific polyclonal IgG. *Semin Nucl Med* 1988;18:335–344.
4. Oyen WJG, Claessens RAMJ, van der Meer JWM, Corstens FHM. Detection of subacute infectious foci with indium-111-labeled autologous leukocyte and indium-111-labeled human nonspecific immunoglobulin G: a prospective, comparative study. *J Nucl Med* 1991;32:1854–1860.
5. Corstens FHM, van der Meer JWM. Imaging inflammation with human polyclonal immunoglobulin: not looked for but discovered [Editorial]. *Eur J Nucl Med* 1992;19:155–158.
6. Boerman OC, Storm G, Oyen WJG, et al. Sterically stabilized liposomes labeled with In-111 to image focal infection. *J Nucl Med* 1995;36:1639–1644.
7. Babich JW, Solomon H, Pike MC, et al. Technetium-99m-labeled hydrazino nicotinamide derivatized chemotactic peptide analogs for imaging focal sites of bacterial infection. *J Nucl Med* 1993;34:1964–1974.
8. Corstens FHM, van der Meer JWM. Chemotactic peptides: new locomotion for imaging of infection? [Editorial]. *J Nucl Med* 1991;32:491–494.
9. Moyer BR, Vallabhajosula S, Lister-James J, et al. Development of a white blood cell specific technetium-99m imaging agent from platelet factor 4 for detecting infection. *J Nucl Med* 1996;37:673–679.
10. Subramanian R, Colony J, Shaban S, et al. New chelating agent for attaching indium-111 to monoclonal antibodies: in vitro and in vivo evaluation. *Bioconjugate Chemistry* 1992;3:248–256.
11. Klein JL, DeJager RL, Stiekema JCJ, et al. Human monoclonal antibodies. Application in radioimmunotherapy. In: Goldenberg DM, ed. *Cancer therapy with radiolabeled antibodies.* Boca Raton, FL: CRC Press; 1995:271–281.
12. Vallabhajosula S, Subramanian R, Palestro CJ, et al. Evaluation of indium-111-labeled immunoglobulins for imaging infection: IgM versus IgG antibodies. *J Nucl Med* 1992;33:1031.
13. Oyen WJG, Boerman OC, et. al, Biodistribution of indium-111-labeled IgG and IgM in experimental infection. *Nucl Med Commun* 1996;17:616–620.
14. Vallabhajosula S, Subramanian R, Zhao QH, et al. Indium-111-LiLo-human monoclonal IgM 16.88, a new tracer for imaging focal infection: comparison of kinetics with indium-111-polyclonal IgG. *Eur J Nucl Med* 1995;22:903.
15. Haspel MV, McCabe RP, Pomato N, et al. Generation of tumor cell reactive human monoclonal antibodies using peripheral blood lymphocytes from actively immunized colorectal carcinoma patients. *Cancer Res* 1985;45:3951–3961.
16. Peters LC, Brandhorst JS, Hanna MG Jr. Preparation of immunotherapeutic autologous tumor cell vaccines from solid tumors. *Cancer Res* 1979;39:1353–1360.
17. Pomato N, Murray JH, Bos E, Haspel MV, McCabe RP, Hanna MG Jr. Identification and characterization of a human colon tumor-associated antigen, CTAA-16.88, recognized by a human monoclonal antibody. In: Metztar RS, Mitchell MS, eds. *Human tumor antigens and specific tumor therapy.* New York, NY: Alan R. Liss; 1989:127–136.
18. Subramanian R, Meares CF. Bifunctional chelating agents for radiometal-labeled monoclonal antibodies. In: Goldenberg DM, ed. *Cancer imaging with radiolabeled antibodies.* Boston: Kluwer Academic; 1990:183–199.
19. Sell S. *Immunology immunopathology and immunity.* 4th ed. New York: Elsevier; 1987.
20. McCabe RP, Haspel MV, Carrasquillo JA, et al. Recent developments and perspectives on the future of human and murine monoclonal antibodies in the diagnosis and treatment of cancer. In: Crommelin DJA, Schellekens H, eds. *From clone to clinic.* Amsterdam: Kluwer; 1990:175–188.
21. Steis RG, Carrasquillo JA, Bookman MA, et al. Toxicity, immunogenicity and tumor radioimmunodetecting ability of two human monoclonal antibodies in patients with metastatic colorectal carcinoma. *J Clin Oncol* 1990;8:476–490.
22. Subramanian R, Klein JL, Williams JR, Song S-Y, Hanna MG Jr. Yttrium-90-labeled human monoclonal antibodies for radioimmunotherapy-preclinical evaluation in rabbits. *Proceedings of the American Association for Cancer Research* 1994;35:527.
23. Halpern SE, Hagen PL, Chen A, et al. Distribution of radiolabeled human and mouse monoclonal IgM antibodies in murine models. *J Nucl Med* 1988;29:1688–1696.
24. Vallabhajosula V, Ali KSM, Goldsmith SJ, et al. Evaluation of technetium-99m-labeled peptides for imaging infection in a rabbit model [Abstract]. *J Nucl Med* 1993;34(suppl):104P.
25. Taddei-Peters WC, Haspel MV, Vente P, et al. Quantitation of human tumor-reactive monoclonal antibody 16.88 in the circulation and localization of 16.88 in colorectal metastatic tumor tissue using murine antiidiotypic antibodies. *Cancer Res* 1992;52:2603–2609.
26. Haisma HJ, Pinedo HM, Dessel, MAP, et al. Human IgM monoclonal antibody 16.88: pharmacokinetics and immunogenicity in colorectal cancer patients. *J Natl Cancer Insti* 1991;83:1813–1819.
27. Klein JL, DeJager RL, McCullers GA, Stiekema JCJ, Subramanian R, Hanna MG Jr. Human antihuman antibody response (HAHA) to injection of ^{99m}Tc-, ^{131}I- and ^{90}Y-labeled human monoclonal antibody. *J Immunother* 1994;16:168.

Three-Dimensional Dosimetry for Intralesional Radionuclide Therapy Using Mathematical Modeling and Multimodality Imaging

Glenn D. Flux, Steve Webb, Robert J. Ott, Sarah J. Chittenden and Robert Thomas

Joint Department of Physics, Institute of Cancer Research and Royal Marsden National Health Service Trust, Downs Road, Sutton, Surrey, SM2 5PT, United Kingdom

A method of dosimetry is described that quantifies the three-dimensional absorbed-dose distribution resulting from an intralesional administration of a radiolabeled monoclonal antibody, allowing for both spatial and temporal heterogeneity of distribution of the radionuclide and without the need for a calibration scan. **Methods:** A mathematical model was developed to describe the distribution of activity as a function of time resulting from infusion at a single point within the solid component of a tumor. The parameters required for this model are either known directly or may be obtained from SPECT image data registered to computed tomography. Convolution of this distribution with a point-source dose kernel enabled the three-dimensional absorbed-dose distribution to be obtained. **Results:** This method was applied to a set of patient data acquired in the course of a clinical study performed at our center, and dose profiles and dose-volume histograms were produced. It was shown that the three-dimensional distribution of dose was significantly nonuniform. **Conclusion:** Initial results suggest that this method offers a means of determining the absorbed dose distribution within a tumor resulting from intralesional infusion. This method extends the Medical Internal Radiation Dose computation, which, in these circumstances, would make erroneous assumptions. Furthermore, it will enable individual patient treatment planning and optimization of the parameters that are within the clinician's control.

Key Words: dosimetry; image registration; glioma; radioimmunotherapy; intralesional therapy

J Nucl Med 1997; 38:1059–1066

Targeted radionuclide therapy, using radiolabeled monoclonal antibodies (MAbs), aims to deliver a therapeutic dose to a tumor while minimizing the dose to nontarget organs. It has been shown that intralesional therapy, whereby the radiopharmaceutical is administered directly into the tumor by means of an